HHS Public Access

Author manuscript

J Magn Reson Imaging. Author manuscript; available in PMC 2021 June 02.

Published in final edited form as:

J Magn Reson Imaging. 2021 February ; 53(2): 333–346. doi:10.1002/jmri.27319.

7T MR Safety

Andrew J. Fagan, PhD[1,*], **Andreas K. Bitz, PhD**[2], **Isabella M. Björkman-Burtscher, MD PhD**[3], **Christopher M. Collins, PhD**[4], **Vera Kimbrell, BSRT (MR)**[5], **Alexander J.E. Raaijmakers, PhD**[6], **ISMRM Safety Committee**

[1]Department of Radiology, Mayo Clinic, Rochester, Minnesota, USA; [2]Faculty of Electrical Engineering and Information Technology, FH Aachen - University of Applied Sciences, Aachen, Germany; [3]Department of Radiology, University of Gothenburg, Sahlgrenska Academy, Sahlgrenska University Hospital, Gothenburg, Sweden; [4]Center for Advanced Imaging Innovation and Research, NYU Langone Medical Center, New York, New York, USA; [5]Department of Radiology, Brigham and Women's Hospital, Boston, Massachusetts, USA; [6]Department of Radiology, UMC Utrecht, Utrecht, The Netherlands

Abstract

Magnetic resonance imaging and spectroscopy (MRI/MRS) at 7T represents an exciting advance in MR technology, with intriguing possibilities to enhance image spatial, spectral, and contrast resolution. To ensure the safe use of this technology while still harnessing its potential, clinical staff and researchers need to be cognizant of some safety concerns arising from the increased magnetic field strength and higher Larmor frequency. The higher static magnetic fields give rise to enhanced transient bioeffects and an increased risk of adverse incidents related to electrically conductive implants. Many technical challenges remain and the continuing rapid pace of development of 7T MRI/MRS is likely to present further challenges to ensuring safety of this technology in the years ahead. The recent regulatory clearance for clinical diagnostic imaging at 7T will likely increase the installed base of 7T systems, particularly in hospital environments with little prior ultrahigh-field MR experience. Informed risk/benefit analyses will be required, particularly where implant manufacturer-published 7T safety guidelines for implants are unavailable. On behalf of the International Society for Magnetic Resonance in Medicine, the aim of this article is to provide a reference document to assist institutions developing local institutional policies and procedures that are specific to the safe operation of 7T MRI/MRS. Details of current 7T technology and the physics underpinning its functionality are reviewed, with the aim of supporting efforts to expand the use of 7T MRI/MRS in both research and clinical environments. Current gaps in knowledge are also identified, where additional research and development are required.

MAGNETIC RESONANCE IMAGING AND SPECTROSCOPY (MRI/MRS) has evolved along a path of increasing magnetic field strength from the first whole-body clinical system developed in the 1970s (40 mT[1]), to the current highest-field whole-body research system (10.5 T[2]). At the time of writing, there are over 80 7T whole-body human systems

[*]Address reprint requests to: A.J.F., 200 First Street SW, Rochester, MN 55905, USA. fagan.andrew@mayo.edu.

worldwide, a growing number of which have regulatory clearance in the USA and Europe for performing clinical diagnostic imaging. MRI and spectroscopy at 7T offers intriguing possibilities to enhance image spatial, spectral, and contrast resolution; the reader is referred to several recent reviews.[3–6] Safety concerns have accompanied this increase in field strength, driven primarily by concerns relating to potential interactions with larger static magnetic fields and higher frequency electromagnetic fields (although the latter is of less concern for nuclei other than ^{1}H due to their lower Larmor frequencies). Solutions to these problems, for example, the use of parallel transmit techniques to reduce specific absorption rate (SAR) and improve image uniformity, present additional safety challenges.[7] The increasing prevalence of implanted electrically conductive devices in patient and research subject cohorts, coupled with the substantive lack of safety testing of such devices to date, further obfuscate the safety concerns for imaging at 7T.

To address these concerns, an International Society for Magnetic Resonance in Medicine (ISMRM)-sponsored Working Group was formed to review the safety aspects specific to 7T MRI/MRS and to identify knowledge gaps where additional research and development is required. The over-arching aim was to provide sufficiently detailed theoretical and practical information to the MR physicists, radiologists, technologists/radiographers, and/or researchers to allow them to make informed decisions relating to the safety of 7T MRI/MRS at their institution, whether in the development of safety procedures or in performing risk/benefit analyses for specific scans. In this, no distinction is made between research and clinical diagnostic environments because, while different considerations and complexity may exist when performing risk/benefit analyses in a research vs. a clinical setting, the underlying safety concerns are the same. A survey sent out to the ultrahigh-field MR community by the Working Group during the summer of 2018 suggest that ~30% of 7T facilities are performing some degree of clinical diagnostic imaging in addition to research activities. This proportion of clinical-to-research imaging is likely to increase significantly as the installed base of regulatory-approved 7T systems expands, particularly in hospital environments with little prior experience of 7T MRI/MRS. The current article thus aims to provide a resource for users of this technology irrespective of the end use. This article was written on behalf of and approved by the ISMRM Safety Committee, and reviewed by the ISMRM Safety and High Field Study Groups.

7T Safety Team Perspectives

At 7T, challenges arise from imaging at the higher frequency of 300 MHz (for ^{1}H) and associated image quality and SAR concerns. The regulatory clearance in 2017 of the first 7T system for clinical diagnostic imaging in the USA and Europe demonstrates how far the technology has progressed. This regulatory clearance followed a critical mass of data in the scientific literature that demonstrated no serious health effects from exposure to static magnetic fields up to 8T,[8] culminating in the 2015 amendment of the International Electrotechnical Commission (IEC) 60601–2–33 standard, which increased the first-level controlled operating mode for the static magnetic field to 8T, effectively matching the Food and Drug Administration (FDA) declaration from 2003 that MRI up to 8T constitutes a nonsignificant risk for adults, children, and infants of 1 month and older. Regulatory guidelines in many other jurisdictions closely follow the IEC standard.

Although 7T MR systems operate within the same general safety framework as conventional systems, they do present a new set of technical, logistical, and oversight challenges, which require a truly multidisciplinary team approach to address this in an efficacious manner. A dedicated 7T Safety Team, comprised of physicists, technologists/radiographers, and radiologists who are knowledgeable with 7T-specific safety issues should be established to articulate policies and procedures that ensure adherence to local regulation and best practice in the field, and to perform risk/benefit analyses for individual cases as required. For institutions with little experience of 7T MRI/MRS, the setting up of such local teams would greatly benefit from a coordinated approach from the 7T MR Community to share knowledge and experiences. The UK7T network[9] and the German Ultrahigh Field Imaging[10] consortia are examples of such initiatives.

The first generation of 7T magnets were large, heavy, and without active shielding, requiring either a significant amount of steel shielding or space to accommodate the large fringe fields, making siting difficult. The latest generations of 7T magnets have significantly less mass and are actively shielded. The large magnet coupled with the lack of vertical table movement on some systems can necessitate lowering the magnet 50–70 cm below floor level to maintain the table at a reasonable height, an important consideration to minimize the risk of injury to a subject falling off the table. A quenching 7T magnet will produce a larger volume of helium gas compared to lower field systems, and take longer to drop to zero field; staff should be trained accordingly, for example, in deciding when after a quench it is safe for firefighters to enter the magnet room (termed “Zone 4” in the American College of Radiology’s MR facility zoning nomenclature[11]).

Physicists, radiologists, and MR technologists/radiographers working at 7T should together be knowledgeable across a number of topics specific to ultrahigh-field, such as the interaction of 300 MHz RF energy with tissue and electrically conductive implants, the more complex SAR modeling employed to supervise SAR_{10g} values (ie, SAR averaged over 10 g of tissue), and how parallel transmit techniques can impact SAR and image quality. The current generations of 7T systems do not by default have an in-built RF body coil, and hence RF-induced heating of tissue touching the inner surface of the magnet bore is not of concern. The scanning of subjects with electrically conductive implants requires particular attention at 7T; this is discussed in more detail below. Further considerations include the relative lack of robust diagnostic imaging protocols, difficulty in translating many imaging pulse sequences from 3T to 7T, altered image contrast, and prevalence of significant image artifacts.

Some logistical issues to consider to ensuring safety at 7T include:

- The local transmit-receive RF coils on 7T systems tend to be heavier than coils found on lower field systems, and the use of a suitable coil cart for the magnet room (Zone 4) for switching coils is recommended.
- In situations where rapid evacuation of a subject from the magnet bore is required, the slow table movement override mechanism should be used; staff should be familiar with the use of this mechanism, and also aware of the severe vestibular activation this may generate in the subject.

- The table cannot be undocked from the magnet on some 7T systems; an MR Conditional slide board and gurney should be available to transfer the subject out of the room in case of emergency.
- Custom-made dielectric pads, typically made from high permittivity perovskite materials, are often used at ultrahigh-fields to improve image uniformity.[12,13] Care should be exercised in strictly following their intended use.
- Ancillary equipment in the magnet room (Zone 4) may need to be positioned further from the isocenter (and hence from the subject) than typical due to the longer magnet bore and greater spatial extent of the fringe field; for example, contrast agent injector pumps, anesthesia workstations, and/or ventilators may require longer tubing than typically used, and care should be exercised to ensure their functionality with the longer tubing lengths.

Further safety concerns accompanying the transition to 7T relate to adverse events and diagnostic acceptability in general. Clinical evaluation of ultrahigh-field is hampered by the small installed base of 7T systems worldwide, which furthermore vary hugely in their technical specifications due to the rapid pace of development of this new technology. There is similar variability in published 7T studies, particularly regarding methods used and/or the diagnostic purpose in question, while subject cohorts also vary widely regarding not just the intended treatment population or clinical condition, but also age, gender, and even disease severity. Varying data source types, outcome measures, and follow-up time, or simply lack of statistical significance: all contribute to a difficulty in making objective assessments of the diagnostic acceptability of 7T imaging data and to develop evidence-based guidelines for its most efficacious use by referring physicians and providers. It is important that radiologists gain familiarity with the altered image features in some sequences and/or anatomical areas at 7T, such as image contrast changes and new or enhanced image artifacts.[14,15] This can further mitigate safety concerns relating to the potential for misdiagnoses.

Subject Selection

A risk/benefit analysis is required, especially for some categories of subjects (eg, those with thermoregulatory compromise, implants, or young children), arbitrated by a medically responsible principal investigator or radiologist. This risk/benefit analysis should ideally have input from the 7T safety team to achieve a maximally informed decision, while furthermore adhering to the specific approval conditions stipulated by the local Institutional Review Board (IRB) in the case of research studies. Risk/benefit assessments should conform to local regulation and ethical considerations, be strictly documented, and never be sidestepped due to a lack of trained personnel, last-minute changes, or ignorance. It is worth noting that all 7T imaging is effectively performed in “First Level Controlled” mode as per IEC 60601–2–33, since $B_0 > 4T$, thus requiring medical supervision.

Specific challenges are also posed by certain subject groups. There are no published studies investigating the safety of pregnancy at 7T. The current regulatory-cleared 7T system imposes a lower weight limit of 30 kg using either RF coil (head or knee), although this is likely to be reduced to 15 kg in the near future for the head. A lack of confidence in

predicting and hence supervising the worst-case local SAR_{10g} across the pediatric population may contribute to this restriction; the availability of a broader range of virtual human pediatric simulation models is required to overcome this limitation. Sedation and anesthesia is possible at 7T, contingent on available equipment for anesthesia and subject monitoring.

Static B_0 and Magnetic Field Gradient Effects

Safety Considerations Relating to the 7T Static Field

The first generations of 7T magnets (typically pre ~2010[16]) were passively shielded with an extensive fringe field that increased the distance from the magnet wherein the risk of a projectile incident was high. More recent 7T magnets are actively shielded, with fringe fields around the edge of the magnet housing of broadly similar, if slightly extended, spatial extent compared to those on modern 3T systems, and with spatial field gradients ($|\nabla B_0|$) also of broadly similar magnitude, as shown in Fig. 1.

Forces on Paramagnetic and Ferromagnetic Objects

Translational forces on unsaturated ferromagnetic objects are broadly similar in the fringe-field region of actively-shielded 7T systems compared to modern lower-field systems, albeit subject to slightly more extended fringe fields. The position where translational forces are at maximum (ie, the position where the magnetic field multiplied by the spatial field gradients is maximum, or $[B_0 \text{ x} |\nabla B_0|]_{max}$) typically occurs within the relatively long bore of these actively-shielded 7T magnets, in fields well above the saturation flux density for iron ($B_s <$ ~2.5T[17]). For example, for the current regulatory-approved 7T system's magnet, a maximum spatial field gradient ($|\nabla B_0|_{max}$) of 12.2 T/m occurs at the bore wall ~1 m from the isocenter, in a field of ~ 5T, resulting in $[B_0 \times |\nabla B_0|]_{max} = 61.1\ T^2/m$. As shown in Table 1, many current lower-field clinical systems have $[B_0 \times |\nabla B_0|]_{max}$ values that approach or even exceed this, particularly for "high field open" (HFO) magnet designs, with respective magnitude of translational forces on paramagnetic and unsaturated ferromagnetic objects at these peak locations. The force due to torque scales linearly with B_0 for these materials, and hence one can expect a factor 2.3 increase within the bore at 7T compared to 3T.

Additional Forces on Conductive Objects

Even if not ferro- or paramagnetic, Lenz forces on electrically conductive objects (such as electrically conductive implants, electrodes, wires) moving through a magnet's spatial field gradients depend on the magnitude of these gradients,[18] and hence are only of greater concern for 7T magnets with $|\nabla B_0|$ values higher than on lower field systems. These effects can be accommodated by reducing the table speed of the magnet (ie, the rate at which the devices are moved through the spatial field gradients).

It is emphasized that the above considerations depend critically on the specifics of the magnet design, and can be expected to change with future 7T magnet designs. In general, accurate knowledge of the static magnetic fields and spatial field gradients in the bore and fringe field areas around a particular system is an essential prerequisite for assessing the potential for dangerous translational and rotational forces that one could encounter acting on

paramagnetic and ferromagnetic objects brought into its vicinity; the system's owner's manual contains such information, and vendors are encouraged to publish such information in a consistent, comparable way.

Safety Considerations Relating to Gradient Switching

Many 7T systems have similar (if not identical) gradient coil configurations as used in lower field strength systems, with typical current maximum gradient magnitudes and slew rates around 80 mT/m and 200 T/m/s, respectively. Consequently, safety concerns relating to peripheral nerve stimulation from gradient switching during imaging are not expected to be of more concern at ultrahigh-fields, although one recent study has reported elevated incidences of peripheral nerve stimulation (PNS) in subjects imaged on an actively-shielded 7T system.[19] It is not clear whether this related specifically to the 7T system used in the study or other methodological factors, but should nevertheless be investigated further to determine the underlying source. Vibrations arising from eddy current-induced torque in highly conducting materials are likely to be increased at 7T, and while these could generate uncomfortable sensations in some subjects (for example, for subjects with cardiac stents, which are not as rigidly held in place as, say, orthopedic implants), further testing is required to determine a potential safety effect. Acoustic noise levels of current 7T systems are broadly similar to 3T systems; in practice, Lorentz damping effects,[20] which reduce acoustic noise levels, offset to some degree the increased Lorentz forces acting on the conductors in the gradient coils. Increased acoustic insulation in the space the body coil would normally occupy and a greater damping mass of the magnet/gradient coil assembly may also help reduce noise, although future magnet designs may have an increased propensity for acoustic noise concerns. Nevertheless, 7T head coils tend to be of tighter design than 3T coils (due to the desire to keep the transmit coil diameter small), making it difficult to use headphones. In these situations, it is crucial that ear plugs of the highest rating possible are used and properly inserted into the external ear canal of subjects. Additional padding should also be used where possible to maximize the amount of hearing protection. New head coil designs that incorporate slim-line headphones with improved audible communication capabilities and active noise cancelling are useful in this regard.

Bioeffects Relating to 7T MRI/MRS

There is no scientific evidence to suggest a long-term bioeffect in humans from exposure to 7T magnetic fields.[21] The maximum translational magnetic and Lorentz forces on current-carrying tissue structures are not of sufficient magnitude at 7T to cause separation of red blood cells from plasma.[22] The Lorentz force is, however, sufficient to cause a large charge separation of positively and negatively charged ions moving in the blood. The resulting electric (E)-field from this magnetohydrodynamic effect alters electrocardiograms (ECG) with an enlarged T-wave, making ECG gating or cardiac monitoring sometimes problematic at 7T. There is no demonstrated safety concern related to blood pressure based on simulation[23] and experimental results[24] up to 10.5T.

A further common bioeffect arising from induced voltages relates to vestibular activation, commonly experienced as a feeling of vertigo, dizziness, and a sense of "moving on a curve" among imaged subjects leading to nausea in extreme cases.[19,25,26] Here, the Lorentz force is

generated by an interaction between normal ionic currents in the inner ear endolymph and the large static and gradient magnetic fields.[27] Movement of the head through these gradient fields, for example, as the table moves in and out of the magnet, and even lying static within a 7T magnet, are thus implicated in activation of the vestibular apparatus. A broad range of such activations has been reported (ranging from 30–85% among imaged subjects[3,19]), most likely due to large variations in magnet design, subject positioning, and/or table speeds. However, surveys conducted postimaging revealed a strong willingness of subjects to undergo repeat imaging, and ancillary evidence of patients imaged clinically at 7T reveal similar levels of tolerance to imaging at lower field strengths.[28] Subjects should be advised to keep their head still at all times, from initial positioning on the table before the exam to removal of the RF coil at the end.

The magnetic fields (static and spatial gradient) around actively shielded 7T magnets only become larger than those on lower field systems close to and within the bore. Staff and subjects should be advised to move their heads slowly in these locations, and staff/researchers should avoid placing their head into the bore whenever possible, for example, when setting up an examination or communicating with subjects already in the bore. If performing activities requiring repair or cleaning within the bore, staff should be mindful of potential transient effects persisting for some time after exposure, and may need to avoid activities such as driving immediately afterwards.[26]

The same recommendations apply to non-MR personnel (eg, anesthesiologists, parents/guardians or caregivers) accompanying subjects into the magnet room (Zone 4), where local policies permit this. Although slow table movements are standard on 7T systems to minimize vestibular activation within subjects, it is recommended that the operator remains in the magnet room and in communication with the subject until the table has reached isocenter. This procedure would ensure that the subject is able to proceed with the imaging examination. Several studies have reported postimaging dizziness and vertigo in subjects in the minutes after a 7T examination,[19] with postural instability persisting up to 5 minutes after exiting the magnet in some cases.[26,27] It is important to ensure that subjects feel no significant residual effects before they are discharged.

Transitory effects such as metallic taste in the mouth and magnetophosphenes are also enhanced at 7T, albeit with lower reported incidences.[19,25] There are conflicting data in the scientific literature reporting possible transient effects on cognition at 7T[29–32]; any effect may be due to disturbance of the vestibular system.[3]

Radiofrequency Effects

General Introduction

The high frequency of the B_1 field for ^1H at 7T affects tissue heating and image homogeneity. The B_1 fields are associated with concomitant RF E-fields that produce electrical currents and RF power absorption in the body, resulting in tissue heating. The strength of these electric fields generally increases with frequency near the surface of the body (where maximum heating usually takes place) for a desired B_1 field strength in a given portion of the body. At the same time, higher frequencies are associated with shorter

wavelengths. At 300 MHz the wavelength of the RF field inside the subject ranges from about 40 cm in fat to 10 cm in fluids, much shorter than the dimensions of the body and the wavelengths at lower field strengths. These shorter wavelengths result in less homogeneous excitation B_1 field distributions arising from regions of constructive and destructive interference, which can lead to signal inhomogeneities and voids.[33]

RF power deposition is constrained for all field strength systems. RF exposure constraints are referenced to limits on tissue temperature (see[34,35]). However, because tissue temperatures are more difficult to predict or measure, alternative constraints are defined in terms of the SAR. SAR is the deposited power divided by the relevant tissue mass, and which can be assessed more reliably. Regulatory limits are given for whole-body SAR, partial-body SAR (averaged over the portion of the body exposed to RF fields), and local SAR (averaged over any 10-g region of tissue). While the IEC states that volume excitation coils will only be subject to relevant limits on whole-body, partial-body, or head SAR, often local SAR limits are also taken into account in making safety determinations for volume coils at ultrahigh-field. In fact, on the current regulatory-cleared system, the 10 g local SAR limits for knee or brain imaging are reached sooner than partial-body/head limits. This is especially true for transmit arrays that may function as either volume coils or local coils, and which can have sparsely distributed elements positioned relatively close to the subject.

Actual SAR levels and distributions depend on the specific RF transmit coil(s), coil driving configuration, RF power delivered, and morphology and body position of the subject in an exam. This is further complicated by the presence of any additional conductive materials within or in contact with the subject, including (but not limited to) tattoos, metal in jewelry or clothing, devices and implants. As reviewed in greater detail below, manufacturers and researchers typically use some combination of experimental measurements and simulations to ensure safe power levels are used for various scenarios and RF coils.[36]

RF Coils in Ultrahigh-Field MRI/MRS

The whole-body birdcage coil as used for excitation in the vast majority of exams at lower field strengths is not practical or effective at 7T for ^{1}H. Rather, the excitation field at 7T is generated by smaller regional volume coils driven by single transmit systems or by arrays of transmit coils driven by multichannel parallel transmit systems, although at the time of writing only the former have regulatory clearance for patient diagnostic imaging.

Almost all commercially-available RF coils for ultrahigh-field MRI/MRS consist of one or more coils of three basic designs: birdcage coil, loop coil, and dipole antenna (for the level of detail in this work, “transverse electromagnetic (TEM) coils” have field patterns similar to birdcage coils, and “stripline elements” or “TEM elements” have field patterns similar to dipoles). Because electrical currents in the body are driven in the direction of the RF electric fields, it can be helpful to understand the general direction of the electric field for each type of coil. Figure 2 illustrates instantaneous field orientations within a large homogeneous phantom for each of these three basic coil types when empty. Blue lines indicate the direction of the B_1-field, and red lines indicate the direction of the E-field. The electric fields near current-carrying elements are typically parallel to the orientation of the element. The birdcage coil has electric fields parallel to B_0 near the rungs, in the transverse direction near

the end rings, and approaching zero E-field at the middle. This field pattern rotates around the central axis of the coil when driven in quadrature, as is most commonly done. Both loop coils and dipoles are typically configured in arrays. For a single loop coil, the E-field follows a loop-like path and oscillates through time. For an array of dipole antennas, the dominant E-field component near each element is typically parallel to the orientation of the element and the B_0 field.

However, placement of a human subject in any coil or array can significantly alter the E-field and associated currents. For example, because electrical currents in the subject can only flow parallel to a nonconductive boundary, the orientation of the electric field within the body near a boundary with air is necessarily parallel to that boundary. This is illustrated in Fig. 3, where simulated field orientations are depicted for a birdcage coil, a loop coil, and dipole antenna in a human model (Duke[37]).

A common configuration for imaging the head or extremities consists of a birdcage volume coil for excitation and an array of loop coils for reception. For example, the most well-known head coil in 7T MRI, depicted in Fig. 4a, consists of a 2-channel birdcage coil for excitation and a 32-channel loop array for signal reception (Nova Medical, Wilmington, MA). Coils with similar configurations are available from various vendors for knee and wrist imaging at 7T (eg, Fig. 4b). For imaging nuclei other than hydrogen (eg, sodium, phosphorous), Larmor frequencies are lower, such that the use of a body-size birdcage coil for X-nuclei applications is feasible.[38] For example, Larmor frequencies for ^{23}Na and ^{31}P are 78.609 and 120.3 MHz, respectively, both lower than for ^{1}H at 3T.

Because the dimensions of the body can be greater than one wavelength at 300 MHz, a volume coil with a given set of currents will produce a field pattern with regions of constructive and destructive interference. This results in inhomogeneous images, often manifest as regions of very low signal across the body region at 7T; this is particularly problematic for the torso.[39] An array of individual coils driven with independent amplitudes and/or phases provides great flexibility in the overall homogeneity and also in which regions of the body the constructive and destructive interferences occur at any one time. In principle, it is possible to produce a homogeneous field across a single given plane in the body at 7T if enough individual transmit coils are available.[40] In practice, however, constraints are imposed by the limited number of transmit elements (typically ≤8 in the head). Thus, while the amplitudes and phases can be adjusted (“static RF shimming”) to produce an excitation field pattern with high intensity in a desired region or organ, this approach will invariably produce weaker fields elsewhere in the imaging plane. Furthermore, the local SAR distribution changes with static RF shimming (Fig. 5). A more advanced approach is to optimize the evolution of these phases and amplitudes over time within one RF pulse. This is performed independently for each channel, and combined with appropriately evolving gradient field patterns, to achieve a desired excitation pattern despite inhomogeneous RF fields at any one time. This is called “dynamic RF shimming”; both static and dynamic RF shimming are referred to as “parallel transmission” or pTx techniques, and certainly both require a pTx-capable system.[41–43] However, such an RF pulse design further complicates the requirements for ensuring safety, as the local SAR distribution in a given subject can vary arbitrarily through time. The necessity of multitransmit arrays for body imaging at 7T[44]

has led to the development of a wide variety of RF coil arrays, some of which are commercially available (eg, Fig. 4c). Multitransmit coils have numerous demonstrated benefits in the knee and head, with one commercially available option (eg, the Nova Medical 8-channel transmit head coil).

Commercially-developed RF coils for 7T MRI are usually supplied to the customer complete with a fully-characterized RF safety assessment for the intended use of the coil, such as the specific RF excitation pattern or anatomical area for which the system SAR supervision algorithm was intended. However, if this is not supplied by the manufacturer, or when dealing with off-label use of the coil or using home-built coils, it is imperative that a thorough assessment of RF safety is conducted by the institution. Hoffmann et al in 2016 outlined safety testing and operational procedures for home-built RF coils,[36] including but not limited to RF safety. An ISMRM working group is currently working on a white paper guideline document on best practices for safety testing of experimental RF hardware.[45]

Simulations for RF Safety Assurance

Numerical simulations provide the best currently-available method for realistic estimation of RF heating throughout the human body within specific MRI coils.[46] Thorough simulations include realistic representation of the specific RF coils used in practice when loaded with a variety of models of different human subjects located at different positions relative to the coil.[37,47,48] Simulation of SAR requires software capable of solving the Maxwell's equations throughout realistically heterogeneous representations of the human body. For performing simulations for 7T MRI in particular, it is important to also include a large portion of the bore due to the ability of RF fields to propagate along the bore at and above this field strength.[49]

Results obtained from numerical methods are approximate solutions of the realistic problem and therefore the simulation models need to be verified before numerical results can be used to perform meaningful safety assessment for in vivo examinations. To this end, calculated spatial distributions of electric and magnetic fields, SAR, and/or temperature can be compared to results from measurements in vivo or in well-defined test configurations with suitable phantoms filled with tissue-simulating liquid. Available measurement techniques use RF field and dosimetric (SAR) probes,[50–52] B_1^+ mapping,[53,54] and/or MR thermometry.[55–57] Deviations noted during the verification procedure between simulations and measurements determine the uncertainty of the numerical results and must be accounted for during the safety assurance process.[36,58–60] A challenge with these approaches is the significantly greater complexity of the human body relative to that achievable in manufactured phantoms. Thus, for example, the funneling of induced currents by muscle structures in the body can lead to temperature hotspots that are not present in homogeneous phantoms and difficult to mimic in more complex anthropomorphic phantoms. For further details on validation procedures and corresponding methods for determination of safety margins, readers are referred to the forthcoming white paper guideline document on best practices for safety testing of experimental RF hardware.[45] The FDA provides guidance on modeling requirements for medical device submissions, which can be helpful when developing safety documentation for IRB approval.[61]

Dielectric Padding

Materials with a high electric permittivity, most often in the form of flexible “dielectric pads” containing water and some concentration of specific ceramic powders, can be strategically placed against the subject to alter the B_1^+ field distribution.[12,13,62] Typically, dielectric pads are positioned to increase the strength of the excitation B_1 field in a nearby area of interest and are useful for minimizing image artifacts.[14] In some cases their use may allow for a reduction of input power to achieve the desired B_1 field strength in the region of interest, resulting in a lower SAR averaged over the exposed region.[63] SAR algorithms and supervision mechanisms on current MR systems do not consider the impact of dielectric pads on changes to the electromagnetic field. The use of pads in a specific configuration should be performed with caution and in consultation with studies on SAR for similar configurations, if available, or with very conservative power limits and, if possible, new experimental or numerical studies of SAR or temperature increase for the configuration desired. Examples include simulations of the effect of dielectric pads on SAR distributions in the head with specific coil configurations at 7T,[63,64] but more work in this area is needed to allow for more generalizable results.

General SAR Considerations for Parallel Transmission

At the time of writing, parallel transmit techniques do not have regulatory clearance for patient diagnostic imaging. Nevertheless, a variety of methods have been developed to accelerate the calculation of field distributions and hence local SAR through time and space in parallel transmit systems. Q matrices contain normalized information on the interaction of the previously-computed electric fields of the individual transmit coil elements and, hence, allow calculation of the instantaneous global and local SAR aspects.[65] Since body models typically contain several million mesh cells, determination of the maximum local SAR for a particular transmit configuration from Q matrices comes with a high computational cost. A compression algorithm with a specified maximum SAR over-estimation can be applied to generate a reduced set of local SAR matrices known as virtual observation points (VOPs).[66,67] Each VOP represents the maximum SAR for a cluster of voxels within the model, overvalued at maximum by the chosen SAR overestimation. Compression factors from 1000 up to 13,000 have been demonstrated, resulting in only a few hundred VOPs for head regions of typical body models.[66]

Because of the reduced complexity of SAR determination, the VOP approach enables rapid SAR determination for pTx-designed RF pulses. Further, multiple configurations with different body positions in the RF coil and/or various body models can be combined into a single VOP dataset. Thus, such multi-scenario VOP models can be used to monitor a broader range of exposure scenarios with a single dataset. In combination with an online RF monitoring system capable of sampling the instantaneous amplitudes and phases in the individual transmit channels, VOP models may in the future be employed to perform a local SAR supervision during MR examinations.[68]

Temperature Simulations

While SAR is the most commonly-used metric for safety assurance in MRI, there is increasing interest in the use of temperature-based approaches. It is generally acknowledged

that tissue temperature is more directly relevant to safety than SAR, and due to the multiple factors affecting temperature, such as perfusion, there is not always good agreement between distributions of SAR and temperature increase.[69–71] At the same time, is it important to acknowledge that calculation of SAR-induced temperature changes requires an additional layer of equations, variables, and uncertainty when compared to calculation of SAR alone. A bio-heat transfer equation, such as the Pennes' equation,[72] is commonly employed to model heat transfer in the human body considering SAR and tissue metabolic rate as local sources of heat, with thermal conduction to neighboring regions, and with moderation by blood perfusion.[73] For exposures with significant whole-body average SAR, it is necessary to also account for a possible increase in core body temperature.[74,75] At typical RF exposure levels in MRI, blood perfusion is the most effective bio-heat mechanism and influences the temperature distribution significantly. Thus, different temperature-dependent blood perfusion models[76,77] have been introduced to account for healthy volunteers as well as volunteers with impaired thermoregulation (eg, diabetics).[48,78] However, validation of perfusion models requires further research.[79]

Verification of in vivo numerical results from thermal simulations is difficult, since the sensitivity of noninvasive 3D temperature mapping techniques, like MR thermometry,[80] is currently not sufficient for any meaningful comparisons. Further, measurements in vivo, even if they are performed by temperature probes at discrete locations in the body, are difficult to use for verification because of the possible difference between thermal regulation (blood perfusion models) in simulation and in vivo.

Electrically Conductive Implants

At the time of writing, only a handful of implant devices have been labeled by the manufacturer as MR Conditional at 7T (predominately otologic and middle ear implants.[81–84] The rapid increase in the numbers of 7T system installations worldwide will hopefully provide an incentive to implant manufacturers to address this deficit.

Static and Spatial Field Gradient Interactions

Several articles have described the magnetic force testing of implants at 7T. These include investigations of stents,[85,86] various orthopedic devices,[86,87] intrauterine devices,[87,88] various dental retainer wires and implants,[89,90] cranial fixation devices,[91] inner ear implants,[92] shunt valves,[93] and hemostatic and intracranial aneurysm clips.[94] In many cases, no significant magnetic forces were measured, although the following did exhibit potentially dangerous effects: two stents,[86] long orthopedic implants,[86] dental magnetic attachment keepers,[90] and some hemostatic/intracranial aneurysm clips.[94] The shunt valves lost the ability to be reprogrammed after exposure to the 7T field.[93] Interestingly, the four vascular grafts assessed in the Feng et al study produced markedly different deflection test results, despite the manufacturer listing them being made from the same materials with comparable structure.[86] This highlights the need to obtain precise information regarding a device's material composition and also the danger in generalizing results to untested devices. A recent article presented magnetic displacement force and torque data for 11 common medical implant alloys,[95] which may assist with information gathering to generate MR

Conditional labeling for devices composed of these specific alloys. Furthermore, deflection angles measured at 3T are at best only a rough indicator of likely deflection angles at 7T. As such, some devices that are imaged as a matter of routine at ≤3T may be unsafe to scan at 7T,[86] and hence it is critical that the MR technologists/radiographers responsible for subject screening are aware of the need for extra vigilance to identify all metallic objects in a subject's body. It is recommended that institutions maintain a database of metallic objects previously imaged, together with the specific circumstances and rationale used to reach the decision. Standardized testing approaches[96,97] can be used to assess potentially hazardous magnetic field forces for any previously untested objects. For such objects successfully imaged and/or tested, the sharing of such information among the ultrahigh-field community would be extremely useful, though not decreasing the local responsibilities. A standardized format for recording such information would help in this regard, with databases modeled on current online resources (such as[98,99]).

RF Interactions

A wide range of conditions can significantly alter the SAR distribution, potentially causing much higher focal RF heating than could be expected otherwise when a given coil is used as intended. This can include the presence of electrically conductive objects or materials, either in contact with or implanted within the subject, such as medical devices and implants, dental appliances, jewelry, clothing with metallic fibers, ECG electrodes/pads, and even pigments in cosmetics and tattoo ink.[100] For these reasons, careful subject screening and handling are critical to ensuring subject safety at 7T, as at any field strength, and manufacturers of medical devices should work to determine conditions under which their products can be imaged without risk to the subject or damage to the device.[101] While experimental measurements of temperature increase in phantoms near implants are essential, recent approaches increasingly also favor simulation-based assessment of the implants in a wide range of possible configurations and human subjects with consideration of SAR and/or temperature.[89,102,103]

The imaging of subjects with implants or nonremovable jewelry or cosmetics (including tattoos, permanent eyeliner, artificial eyelashes, etc.) must be approached with caution. In addition to the significant increase in local SAR for a given imaging sequence at higher B_0 field strengths, shorter RF wavelengths and different RF field distributions at 7T add another layer of complexity to heating patterns and safety.

The limited number of publications including RF heating data of passive implants at 7T currently includes reports of a variety of simulations and in vitro experimental measurements for: stents[85,102,104]; aneurysm clips[94,103,105]; cranial plates, covers, and fixation devices[91,106,107]; intrauterine devices (IUDs)[88,108]; dental implants[89]; orthopedic fixation devices[86]; and electroencephalogram leads.[109] The conditions for simulation and experiment vary widely, but for most cases the source of RF energy is a volumetric head coil or equivalent, and the maximum local SAR or rate of temperature increase when the device is located in a region of high local SAR is seen to be some multiple of the value for the case with no implant present, such that some safety factor for imaging a subject with such an implant in such a coil might be discerned, provided the placement of the device is similar to

that in the reported study. Exceptions include simulations of a cardiac stent in different transmit arrays for imaging the torso, which shows that, indeed, coil design and drive configuration are additional major considerations for ensuring safety in such a situation.[102] The proximity of different devices to each other can be a complicating factor. Also, when implants have narrow geometrical features, regions of very focal SAR may be present, reducing the usefulness of SAR averaged over a predefined mass or volume of tissue (ie, 10 g- or 1 g-averaged) compared to limiting temperature instead.[102,103,110] Thermal simulations can provide direct information on tissue temperature and allow for consideration of realistic tissue distributions and effects on heat transfer from blood perfusion. More work is clearly required in this area. Nevertheless, the important role of RF and thermal simulation in implant safety is reflected in current safety standards.[111]

General factors that can affect the likelihood of significant heating of a passive implant include position and size of the implant. In general, smaller implants, implants far from the source of RF energy (eg, located in the lower extremity during an exam with a head-specific transmit coil), and implants oriented with their longest dimension perpendicular to the electric field are less likely to experience significant RF heating. The actual electric field distribution depends very much on the local anatomy, and hence is difficult to predict. Because RF wavelengths are shorter at 7T than lower field strengths, the size of implants that can be imaged without considering the complicating effects of wavelength is much smaller at 7T. One study reviewed survey data on 230 subjects having some sort of implant who had been imaged at 7T with attention to size of the implant and distance from the source of RF energy.[87] No subjects reported RF heating effects under their criteria, which allowed for passive nonmagnetic electrically conductive implants more than 30 cm from the end of the coil as long as they were also shorter than one wavelength, although it should be noted that it is expected that a potential for maximum in heating occurs in straight conductors about half that length. Implants closer to the coil or within the imaging region require a greater level of a priori knowledge. Long conductors are less likely to carry significant current if they are perpendicular to the applied electric fields. However, the E-field orientation with respect to an implant within a subject cannot be known, since this orientation varies at different locations within the coil and also within the subject. One must therefore consider the worst-case scenario of the E-field parallel to the implant.[103] There is ongoing research on deliberately exciting birdcage coils and transmit arrays such that an implant would be in a region of low electric field.[112]

There are currently no data on imaging subjects with active implants at 7T. Given the higher B_1 frequency at 7T, subjects with active implants in place or operational should generally not be imaged at 7T until additional data specific to the particular device at 7T are available.

Conclusion

The growing history of the safe use of 7T MRI/MRS bodes well for the translation of this technology into the clinical arena and its continued use as a clinical and scientific research tool. There remain, however, several gaps in knowledge, and hence opportunities for fruitful scientific investigations, particularly with regard to techniques such as parallel transmission and SAR/temperature modeling.

It is important to emphasize the importance of having the requisite knowledge within the 7T Safety Team to make informed decisions on safety; for example, if performing off-label imaging on a commercial system or when using home-built RF coils. This of course also applies to lower field systems, but is perhaps more pertinent at 7T considering the relatively more complex interactions of the higher-frequency RF energy with tissue and implants. While each site has ultimate responsibility for the use of their 7T system, the responsible physician or principal investigator should take all available sources of information into account when making safety assessments related to imaging at 7T.

Summary of Main Recommendations

The following list summarizes the main recommendations outlined in this article relating to ensuring safety for 7T MRI/MRS. It is emphasized that safety at 7T is subject to the same considerations that apply at lower magnetic field strengths, and hence these recommendations should be seen as additional to standard MRI/MRS safety procedures.

Set-up multidisciplinary 7T safety team:

develop policies and procedures that address issues specific to 7T imaging

- Clear guidance for those categories of subjects who may be imaged
  - Clinical indications for the exam
  - Presence of implants and the process for researching and clearing
  - Subject’s physiological status and weight
  - What requires a risk/benefit analysis on individual subjects and the procedure to do so
- Outline of institutional policy on off-label imaging
  - Most implants are currently untested at 7T and therefore are “off-label” for imaging
  - Similarly, many 7T systems are not regulatory cleared
  - pTx methods currently are not regulatory cleared
  - the use of RF coils for imaging anatomical areas not included in their regulatory-clearance is “off-label”
- Policies for managing personnel and subjects regarding vestibular effects
- Establish and train on safety procedures for emergencies including magnet quench

Information needed to support safety team and in establishing procedures:

- Ensure accurate knowledge of the system’s magnetic field profile (static field and spatial field gradients) in the bore and fringe field regions, as this can help guide the risk/benefit assessment

- Ensure thorough assessment of the safety of all RF coils used with the system, particularly home-built coils, research hardware, and ancillary equipment
- Each facility may wish to maintain a database of implanted devices imaged and those internally tested by local personnel

Items requiring further research and investigation:

- Evaluate the safety of imaging subjects with electrically conductive implants, including magnetic field forces and RF-induced tissue heating
- Investigate the safe and optimal use of high permittivity materials (ie, dielectric pads) within the RF coil for improving B_1 field distributions
- Investigate modified RF excitation patterns in birdcage and transmit array coils to reduce the resultant E-field at an implant location
- Investigate imaging during pregnancy and of young children and neonates
- Validate Q matrix and VOP models for determining SAR levels with parallel transmit techniques
- Validate blood perfusion models for temperature-based simulation approaches to RF safety

Acknowledgments

The authors acknowledge the many useful comments from members of the ISMRM Safety Committee, the High Field Safety Group, and the High Field Study Group, in particular Michael Steckner, Johan van den Brink, Scott Reeder, Vikas Gulani, Greg Metzger, Benedikt Poser, and Karin Markenroth Bloch.

REFERENCES

1. Hutchinson JMS, Edelstein WA, Johnson G. A whole-body NMR imaging machine. J Phys E 1980;13(9):947–955.
2. He X, Erturk MA, Grant A, et al. First in-vivo human imaging at 10.5T: Imaging the body at 447 MHz. Magn Reson Med 2020;84:289–303. [PubMed: 31846121]
3. Ladd ME, Bachert P, Meyerspeer M, et al. Pros and cons of ultra-high-field MRI/MRS for human application. Prog Nucl Magn Reson Spectrosc 2018;109:1–50. [PubMed: 30527132]
4. Obusez EC, Lowe M, Oh SH, et al. 7T MR of intracranial pathology: Preliminary observations and comparisons to 3T and 1.5T. Neuroimage 2018;168:459–476. [PubMed: 27915116]
5. Trattnig S, Springer E, Bogner W, et al. Key clinical benefits of neuroimaging at 7T. Neuroimage 2018;168:477–489. [PubMed: 27851995]
6. Henning A. Proton and multinuclear magnetic resonance spectroscopy in the human brain at ultra-high field strength: A review. Neuroimage 2018;168:181–198. [PubMed: 28712992]
7. Padormo F, Beqiri A, Hajnal JV, Malik SJ. Parallel transmission for ultrahigh-field imaging. NMR Biomed 2016;29(9):1145–1161. [PubMed: 25989904]
8. Amendment to the ICNIRP “statement on medical magnetic resonance (MR) procedures: Protection of patients”. Health Phys 2009;97(3):259–261. [PubMed: 19667810]
9. www.uk7t.org/.
10. mr-gufi.de/index.php/en/about-gufi/.
11. Kanal E, Barkovich AJ, Bell C, et al. ACR guidance document on MR safe practices: 2013. J Magn Reson Imaging 2013;37(3):501–530. [PubMed: 23345200]

12. Teeuwisse WM, Brink WM, Haines KN, Webb AG. Simulations of high permittivity materials for 7T neuroimaging and evaluation of a new barium titanate-based dielectric. Magn Reson Med 2012;67(4):912–918. [PubMed: 22287360]
13. Webb AG. Dielectric materials in magnetic resonance. Concept Magn Reson A 2011;38A(4):148–184.
14. Fagan AJ, Welker KM, Amrami KK, et al. Image artifact management for clinical magnetic resonance imaging on a 7T scanner using single-channel radiofrequency transmit mode. Invest Radiol 2019;54(12):781–791. [PubMed: 31503079]
15. Barisano G, Sepehrband F, Ma S, et al. Clinical 7T MRI: Are we there yet? A review about magnetic resonance imaging at ultra-high field. Br J Radiol 2019;92(1094):20180492. [PubMed: 30359093]
16. van Osch MJP, Webb AG. Safety of ultra-high field MRI: What are the specific risks? Current Radiology Reports 2014;2(61):1–8.
17. Panych LP, Madore B. The physics of MRI safety. J Magn Reson Imaging 2018;47(1):28–43. [PubMed: 28543948]
18. Condon B, Hadley DM. Potential MR hazard to patients with metallic heart valves: The Lenz effect. J Magn Reson Imaging 2000;12(1):171–176. [PubMed: 10931577]
19. Hansson B, Höglund P, Markenroth Bloch K, et al. Short-term effects experienced during examinations in an actively shielded 7 T MR. Bio-electromagnetics 2019;40(4):234–249.
20. Winkler SA, Alejski A, Wade T, McKenzie CA, Rutt BK. On the accurate analysis of vibroacoustics in head insert gradient coils. Magn Reson Med 2017;78(4):1635–1645. [PubMed: 27859549]
21. Fatahi M, Reddig A, GCB V, et al. DNA double-strand breaks and micronuclei in human blood lymphocytes after repeated whole body exposures to 7T magnetic resonance imaging. Neuroimage 2016;133: 288–293. [PubMed: 26994830]
22. Schenck JF. Safety of strong, static magnetic fields. J Magn Reson Imaging 2000;12(1):2–19. [PubMed: 10931560]
23. Keltner JR, Roos MS, Brakeman PR, Budinger TF. Magnetohydrodynamics of blood flow. Magn Reson Med 1990;16(1):139–149. [PubMed: 2255234]
24. Eryaman Y, Zhang P, Utecht L, et al. Investigating the physiological effects of 10.5 Tesla static field exposure on anesthetized swine. Magn Reson Med 2018;79(1):511–514. [PubMed: 28342176]
25. Rauschenberg J, Nagel AM, Ladd SC, et al. Multicenter study of subjective acceptance during magnetic resonance imaging at 7 and 9.4 T. Invest Radiol 2014;49(5):249–259. [PubMed: 24637589]
26. Theysohn JM, Kraff O, Eilers K, et al. Vestibular effects of a 7 Tesla MRI examination compared to 1.5 T and 0 T in healthy volunteers. PLoS One 2014;9(3):e92104. [PubMed: 24658179]
27. Ward BK, Otero-Millan J, Jareonsettasin P, Schubert MC, Roberts DC, Zee DS. Magnetic vestibular stimulation (MVS) as a technique for understanding the Normal and diseased labyrinth. Front Neurol 2017; 8:122. [PubMed: 28424657]
28. Hansson B, Markenroth Bloch K, Owman T, et al. Subjectively reported effects experienced in an actively shielded 7T MRI: A large-scale study. J Magn Reson Imaging 2020. 10.1002/jmri.27139.
29. van Nierop LE, Slottje P, van Zandvoort MJ, de Vocht F, Kromhout H. Effects of magnetic stray fields from a 7 Tesla MRI scanner on neuro-cognition: A double-blind randomised crossover study. Occup Environ Med 2012;69(10):759–766. [PubMed: 22930737]
30. van Nierop LE, Slottje P, van Zandvoort M, Kromhout H. Simultaneous exposure to MRI-related static and low-frequency movement-induced time-varying magnetic fields affects neurocognitive performance: A double-blind randomized crossover study. Magn Reson Med 2015;74(3):840–849. [PubMed: 25224577]
31. Chakeres DW, de Vocht F. Static magnetic field effects on human subjects related to magnetic resonance imaging systems. Prog Biophys Mol Biol 2005;87(2–3):255–265. [PubMed: 15556664]
32. Heinrich A, Szostek A, Meyer P, et al. Cognition and sensation in very high static magnetic fields: A randomized case-crossover study with different field strengths. Radiology 2013;266(1):236–245. [PubMed: 23091174]

33. Van de Moortele PF, Akgun C, Adriany G, et al. B(1) destructive interferences and spatial phase patterns at 7T with a head transceiver array coil. Magn Reson Med 2005;54(6):1503–1518. [PubMed: 16270333]
34. International Electrotechnical Commission (IEC) 60601-2-33 Medical Electrical Equipment - Part 2-33: Particular requirements for the basic safety and essential performance of magnetic resonance equipment for medical diagnosis, Edition 3.2. 2015.
35. Guidelines for Limiting Exposure to Electromagnetic Fields (100 kHz to 300 GHz). Health Phys 2020;118(5):483–524. [PubMed: 32167495]
36. Hoffmann J, Henning A, Giapitzakis IA, et al. Safety testing and operational procedures for self-developed radiofrequency coils. NMR Biomed 2016;29(9):1131–1144. [PubMed: 25851551]
37. Gosselin MC, Neufeld E, Moser H, et al. Development of a new generation of high-resolution anatomical models for medical device evaluation: The virtual population 3.0. Phys Med Biol 2014;59(18):5287–5303. [PubMed: 25144615]
38. Valkovic L, Dragonu I, Almujayyaz S, et al. Using a whole-body 31P birdcage transmit coil and 16-element receive array for human cardiac metabolic imaging at 7T. PLoS One 2017;12(10):e0187153. [PubMed: 29073228]
39. Vaughan JT, Snyder CJ, DelaBarre LJ, et al. Whole-body imaging at 7T: Preliminary results. Magn Reson Med 2009;61(1):244–248. [PubMed: 19097214]
40. Mao W, Smith MB, Collins CM. Exploring the limits of RF shimming for high-field MRI of the human head. Magn Reson Med 2006;56(4): 918–922. [PubMed: 16958070]
41. Zhu Y. Parallel excitation with an array of transmit coils. Magn Reson Med 2004;51(4):775–784. [PubMed: 15065251]
42. Katscher U, Bornert P, Leussler C, van den Brink JS. Transmit SENSE. Magn Reson Med 2003;49(1):144–150. [PubMed: 12509830]
43. Malik SJ, Keihaninejad S, Hammers A, Hajnal JV. Tailored excitation in 3D with spiral nonselective (SPINS) RF pulses. Magn Reson Med 2012;67(5):1303–1315. [PubMed: 21842503]
44. Erturk MA, Li X, Van de Moortele PF, Ugurbil K, Metzger GJ. Evolution of UHF body imaging in the human torso at 7T: Technology, applications, and future directions. Top Magn Reson Imaging 2019;28(3):101–124. [PubMed: 31188271]
45. ISMRM Working Group. Best Practices for Safety Testing of Experimental RF Hardware. Accessed on January 8, 2020. Available from: https://www.ismrm.org/working-groups/best-practices-for-safety-testing-of-experimental-rf-hardware/
46. Fiedler TM, Ladd ME, Bitz AK. SAR simulations & safety. Neuroimage 2018;168:33–58. [PubMed: 28336426]
47. Makris N, Angelone L, Tulloch S, et al. MRI-based anatomical model of the human head for specific absorption rate mapping. Med Biol Eng Comput 2008;46(12):1239–1251. [PubMed: 18985401]
48. Fiedler TM, Ladd ME, Bitz AK. RF safety assessment of a bilateral four-channel transmit/receive 7 Tesla breast coil: SAR versus tissue temperature limits. Med Phys 2017;44(1):143–157. [PubMed: 28102957]
49. Wolf S, Diehl D, Gebhardt M, Mallow J, Speck O. SAR simulations for high-field MRI: How much detail, effort, and accuracy is needed? Magn Reson Med 2013;69(4):1157–1168. [PubMed: 22611018]
50. Weidemann G, Seifert F, Hoffmann W, Pfeiffer H, Seemann R, Ittermann B. Measurements of RF power reflected and radiated by multichannel transmit MR coils at 7T. Magma 2016;29(3):371–378. [PubMed: 27038936]
51. Neufeld E, Kuhn S, Szekely G, Kuster N. Measurement, simulation and uncertainty assessment of implant heating during MRI. Phys Med Biol 2009;54(13):4151–4169. [PubMed: 19521007]
52. Bottauscio O, Cassara AM, Hand JW, et al. Assessment of computational tools for MRI RF dosimetry by comparison with measurements on a laboratory phantom. Phys Med Biol 2015;60(14):5655–5680. [PubMed: 26147075]
53. Morrell GR, Schabel MC. An analysis of the accuracy of magnetic resonance flip angle measurement methods. Phys Med Biol 2010;55(20): 6157–6174. [PubMed: 20876970]

54. Sacolick LI, Wiesinger F, Hancu I, Vogel MW. B1 mapping by Bloch-Siegert shift. Magn Reson Med 2010;63(5):1315–1322. [PubMed: 20432302]
55. Quesson B, de Zwart JA, Moonen CT. Magnetic resonance temperature imaging for guidance of thermotherapy. J Magn Reson Imaging 2000;12(4):525–533. [PubMed: 11042633]
56. Sprinkhuizen SM, Bakker CJ, Bartels LW. Absolute MR thermometry using time-domain analysis of multi-gradient-echo magnitude images. Magn Reson Med 2010;64(1):239–248. [PubMed: 20577981]
57. Simonis FF, Petersen ET, Bartels LW, Lagendijk JJ, van den Berg CA. Compensating for magnetic field inhomogeneity in multigradient-echo-based MR thermometry. Magn Reson Med 2015;73(3):1184–1189. [PubMed: 24664621]
58. Restivo M, Raaijmakers A, van den Berg C, Luijten P, Hoogduin H. Improving peak local SAR prediction in parallel transmit using in situ S-matrix measurements. Magn Reson Med 2017;77(5):2040–2047. [PubMed: 27173968]
59. Massire A, Bitz AK, Boulant N, et al. An 8Tx/8Rx coil validation workflow toward virtual observation points-based parallel transmission cervical spinal cord in vivo imaging at 7T. In: Proc 25th Annual Meeting ISMRM, Honolulu; 2017. p 0477.
60. Ferrand GLM; Amadon A; Boulant N Mathematical tools to define SAR margins for phased Array coil in-vivo applications given E-field uncertainties In: Proc 23rd Annual Meeting ISMRM, Toronto; 2015. p 1862.
61. FDA guidance document, Reporting of computational modeling studies in medical device submissions, FDA-2013-D-1530, 9 2016.
62. Vaidya MV, Deniz CM, Collins CM, Sodickson DK, Lattanzi R. Manipulating transmit and receive sensitivities of radiofrequency surface coils using shielded and unshielded high-permittivity materials. Magma 2018;31(3):355–366. [PubMed: 29110240]
63. O'Brien KR, Magill AW, Delacoste J, et al. Dielectric pads and low- B1 + adiabatic pulses: Complementary techniques to optimize structural T1 whole-brain MP2RAGE scans at 7 Tesla. J Magn Reson Imaging 2014;40(4):804–812. [PubMed: 24446194]
64. Vaidya MV, Lazar M, Deniz CM, et al. Improved detection of fMRI activation in the cerebellum at 7T with dielectric pads extending the imaging region of a commercial head coil. J Magn Reson Imaging 2018;48(2):431–440. [PubMed: 29357200]
65. Graesslin I, Homann H, Biederer S, et al. A specific absorption rate prediction concept for parallel transmission MR. Magn Reson Med 2012;68(5):1664–1674. [PubMed: 22231647]
66. Eichfelder G, Gebhardt M. Local specific absorption rate control for parallel transmission by virtual observation points. Magn Reson Med 2011;66(5):1468–1476. [PubMed: 21604294]
67. Lee J, Gebhardt M, Wald LL, Adalsteinsson E. Local SAR in parallel transmission pulse design. Magn Reson Med 2012;67(6):1566–1578. [PubMed: 22083594]
68. Gumbrecht R, Fontius U, Adolf H, et al. Online local SAR supervision for transmit arrays at 7T. In: Proc 21st Annual Meeting ISMRM, Salt Lake City; 2013.; p 4420.
69. Collins CM, Liu W, Wang J, et al. Temperature and SAR calculations for a human head within volume and surface coils at 64 and 300 MHz. J Magn Reson Imaging 2004;19(5):650–656. [PubMed: 15112317]
70. Wang Z, Lin JC, Mao W, Liu W, Smith MB, Collins CM. SAR and temperature: Simulations and comparison to regulatory limits for MRI. J Magn Reson Imaging 2007;26(2):437–441. [PubMed: 17654736]
71. Massire A, Cloos MA, Luong M, et al. Thermal simulations in the human head for high field MRI using parallel transmission. J Magn Reson Imaging 2012;35(6):1312–1321. [PubMed: 22241685]
72. Pennes HH. Analysis of tissue and arterial blood temperatures in the resting human forearm. J Appl Physiol 1948;1(2):93–122. [PubMed: 18887578]
73. Hasgall PA DF, Baumgartner C, Neufeld E, Lloyd B, Gosselin MC, Payne D, Klingenböck A, Kuster N IT'IS database for thermal and electromagnetic parameters of biological tissues, Version 4.0. DOI:1013099/VIP21000-04-0, itisswiss/database 2018.
74. Shrivastava D, Vaughan JT. A generic bioheat transfer thermal model for a perfused tissue. J Biomech Eng 2009;131(7):074506. [PubMed: 19640142]

75. Carluccio G, Bruno M, Collins CM. Predicting long-term temperature increase for time-dependent SAR levels with a single short-term temperature response. Magn Reson Med 2016;75(5):2195–2203. [PubMed: 26096947]
76. Laakso I, Hirata A. Dominant factors affecting temperature rise in simulations of human thermoregulation during RF exposure. Phys Med Biol 2011;56(23):7449–7471. [PubMed: 22080753]
77. Wang Z, Lin JC, Vaughan JT, Collins CM. Consideration of physiological response in numerical models of temperature during MRI of the human head. J Magn Reson Imaging 2008;28(5):1303–1308. [PubMed: 18972342]
78. Murbach M, Neufeld E, Capstick M, et al. Thermal tissue damage model analyzed for different whole-body SAR and scan durations for standard MR body coils. Magn Reson Med 2014;71(1):421–431. [PubMed: 23413107]
79. Simonis FF, Petersen ET, Lagendijk JJ, van den Berg CA. Feasibility of measuring thermoregulation during RF heating of the human calf muscle using MR based methods. Magn Reson Med 2016;75(4):1743–1751. [PubMed: 25977138]
80. Streicher MN, Schafer A, Ivanov D, et al. Fast accurate MR thermometry using phase referenced asymmetric spin-echo EPI at high field. Magn Reson Med 2014;71(2):524–533. [PubMed: 23440917]
81. Kurz Medical Inc. MR Information. Accessed on January 8, 2020. Available from: https://www.kurzmed.com/en/certificates?file=files/media/MR-Information/MR_Information_en_Rev_06.pdf.
82. Grace Medical Inc. Magnetic Resonance Imaging (MRI) Information for Grace Medical Otologic Implants. Accessed April 19, 2019. Available from: http://www.gracemedical.com/mri-info/.
83. Novatech, Titanium Tracheal Support for Tracheopexy. Accessed on January 8, 2020. Available from: https://www.novatech.fr/nc/en/ent-products/novatechr-tts.html?cid=3328&did=2407&sechash=00d0303c.
84. Corp Glaukos. “iStent inject trabecular micro-bypass system”. Accessed on January 8, 2020. Available from: https://www.glaukos.com/wp-content/uploads/2016/05/45-0119-Rev-2-FINAL-ARTWORK-G2-M-IS-AS-IFU-vendor.pdf.
85. Ansems J, van der Kolk AG, Kroeze H, et al. MR imaging of patients with stents is safe at 7.0 Tesla. In: Proc 20th Annual Meeting ISMRM, Melbourne; 2012. p 2764.
86. Feng DX, McCauley JP, Morgan-Curtis FK, et al. Evaluation of 39 medical implants at 7.0 T. Br J Radiol 2015;88(1056):20150633. [PubMed: 26481696]
87. Noureddine Y, Bitz AK, Ladd ME, et al. Experience with magnetic resonance imaging of human subjects with passive implants and tattoos at 7T: A retrospective study. Magma 2015;28(6):577–590. [PubMed: 26410044]
88. Rauschenberg J, Groebner J, Semmier W, Bock M. How safe are intrauterine devices at MRI procedures with field strengths beyond 1.5T? In: Proc 19th Annual Meeting ISMRM, Montreal; 2011. p 1793.
89. Wezel J, Kooij BJ, Webb AG. Assessing the MR compatibility of dental retainer wires at 7 Tesla. Magn Reson Med 2014;72(4):1191–1198. [PubMed: 24408149]
90. Oriso K, Kobayashi T, Sasaki M, Uwano I, Kihara H, Kondo H. Impact of the static and radiofrequency magnetic fields produced by a 7T MR imager on metallic dental materials. Magn Reson Med Sci 2016;15(1): 26–33. [PubMed: 25994037]
91. Chen B, Schoemberg T, Kraff O, et al. Cranial fixation plates in cerebral magnetic resonance imaging: A 3 and 7 Tesla in vivo image quality study. Magma 2016;29(3):389–398. [PubMed: 27026243]
92. Thelen A, Bauknecht HC, Asbach P, Schrom T. Behavior of metal implants used in ENT surgery in 7Tesla magnetic resonance imaging. Eur Arch Otorhinolaryngol 2006;263(10):900–905. [PubMed: 16835741]
93. Wrede KH, Chen B, Sure U, Quick HH, Kraff O. Safety and function of programmable ventriculo-peritoneal shunt valves: an in vitro 7Tesla: Magnetic Resonance Imaging Study. In: Proc 25th Annual Meeting ISMRM, Honolulu; 2017. p 584.

94. Dula AN, Virostko J, Shellock FG. Assessment of MRI issues at 7T for 28 implants and other objects. AJR Am J Roentgenol 2014;202(2): 401–405. [PubMed: 24450683]

95. Woods T, Delfino J, Rajan S. Assessment of magnetically induced displacement force and torque on metal alloys used in medical devices. ASTM International, J Test Eval 2019. 10.1520/JTE20190096.

96. ASTM F2052–15 Standard test method for measurement of magnetically induced displacement force on medical devices in the magnetic resonance environment. ASTM Int 2015.

97. ASTM F2213–2017, Standard test method for measurement of magnetically induced torque on medical devices in the magnetic resonance environment. ASTM Int 2017.

98. Accessed on January 8, 2020. Available from: www.mrisafety.com.

99. Accessed on January 8, 2020. Available from: magresource.com

100. Hardy PT 2nd, Weil KM A review of thermal MR injuries. Radiol Technol 2010;81(6):606–609. [PubMed: 20606054]

101. Delfino JW, Woods TO. New developments in standards for MRI safety testing of medical devices. Curr Radiol Rep 2016;4:28.

102. Winter L, Oberacker E, Ozerdem C, et al. On the RF heating of coronary stents at 7.0 Tesla MRI. Magn Reson Med 2015;74(4):999–1010. [PubMed: 25293952]

103. Noureddine Y, Kraff O, Ladd ME, et al. In vitro and in silico assessment of RF-induced heating around intracranial aneurysm clips at 7 Tesla. Magn Reson Med 2018;79(1):568–581. [PubMed: 28266079]

104. Santoro D, Winter L, Muller A, et al. Detailing radio frequency heating induced by coronary stents: A 7.0 Tesla magnetic resonance study. PLoS One 2012;7(11):e49963. [PubMed: 23185498]

105. Ibrahim TS, Tang L, Kangarlu A, Abraham R. Electromagnetic and modeling analyses of an implanted device at 3 and 7 Tesla. J Magn Reson Imaging 2007;26(5):1362–1367. [PubMed: 17969135]

106. Kraff O, Wrede KH, Schoemberg T, et al. MR safety assessment of potential RF heating from cranial fixation plates at 7T. Med Phys 2013;40(4):042302. [PubMed: 23556915]

107. Sammet CL, Yang X, Wassenaar PA, et al. RF-related heating assessment of extracranial neurosurgical implants at 7T. Magn Reson Imaging 2013;31(6):1029–1034. [PubMed: 23643158]

108. Sammet S, Koch RM, Murrey DA, Knopp MV. MR-safety and compatibility of intrauterine devices at 3T and 7T. In: Proc 15th Annual Meeting ISMRM, Berlin; 2007. p 1075.

109. Angelone LM, Vasios CE, Wiggins G, Purdon PL, Bonmassar G. On the effect of resistive EEG electrodes and leads during 7T MRI: Simulation and temperature measurement studies. Magn Reson Imaging 2006;24(6):801–812. [PubMed: 16824975]

110. Destruel A, O'Brien K, Jin J, Liu F, Barth M, Crozier S. Adaptive SAR mass-averaging framework to improve predictions of local RF heating near a hip implant for parallel transmit at 7T. Magn Reson Med 2019; 81(1):615–627. [PubMed: 30058186]

111. United States Food and Drug Administration, Assessment of Radiofrequency-Induced Heating in the Magnetic Resonance (MR) Environment for Multi-Configuration Passive Medical Devices. 2016.

112. Eryaman Y, Akin B, Atalar E. Reduction of implant RF heating through modification of transmit coil electric field. Magn Reson Med 2011;65(5):1305–1313. [PubMed: 21500259]

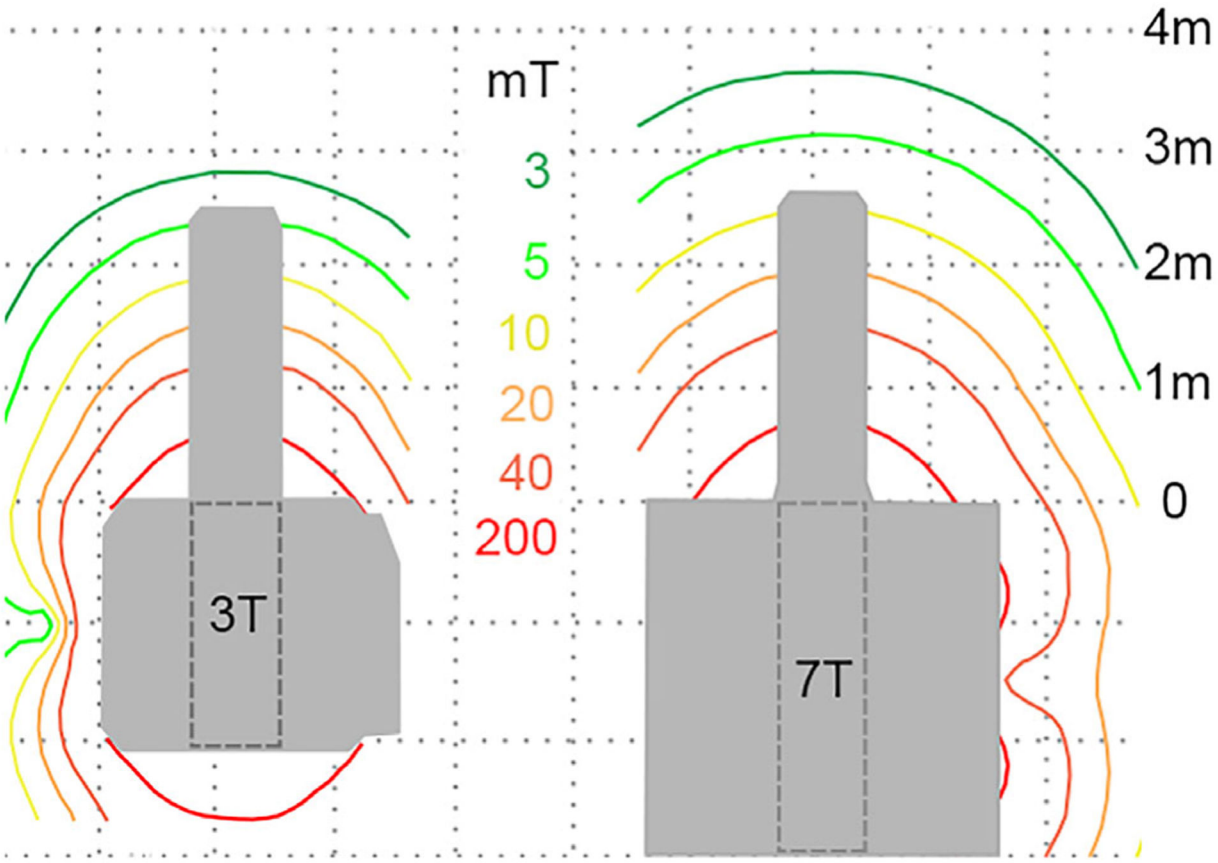

FIGURE 1:
Comparison of the magnetic fringe field for actively-shielded 3T (Prisma, Siemens Medical Systems, Erlangen, Germany) and 7T (Terra, Siemens Medical Systems) systems, demonstrating the similar spatial extent of the static field and spatial field gradients in the area outside of the magnet bore.

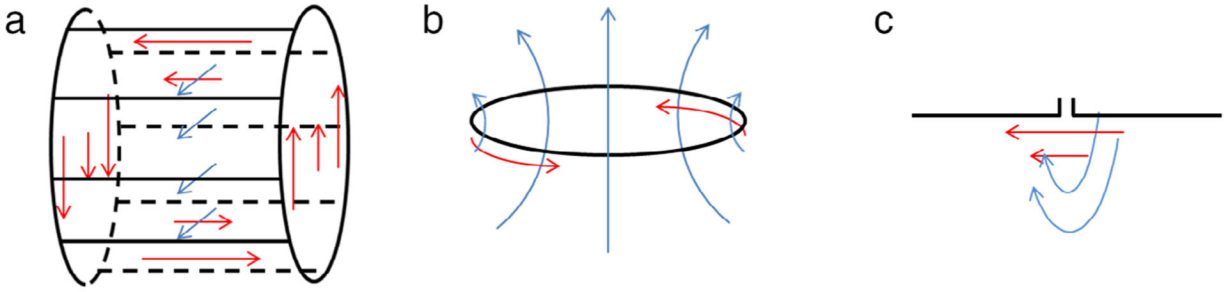

FIGURE 2:

Schematic illustration of basic RF coil structures and instantaneous field patterns for fundamental coil structures when empty: (**a**) birdcage coil, (**b**) loop coil, and (**c**) dipole antenna. Black lines indicate conductor paths, blue lines indicate the direction of the B_1 field, and red lines indicate the direction of the electric field. The field pattern of the birdcage coil rotates about the coil's central axis while that of the loop and dipole would oscillate at the Larmor frequency.

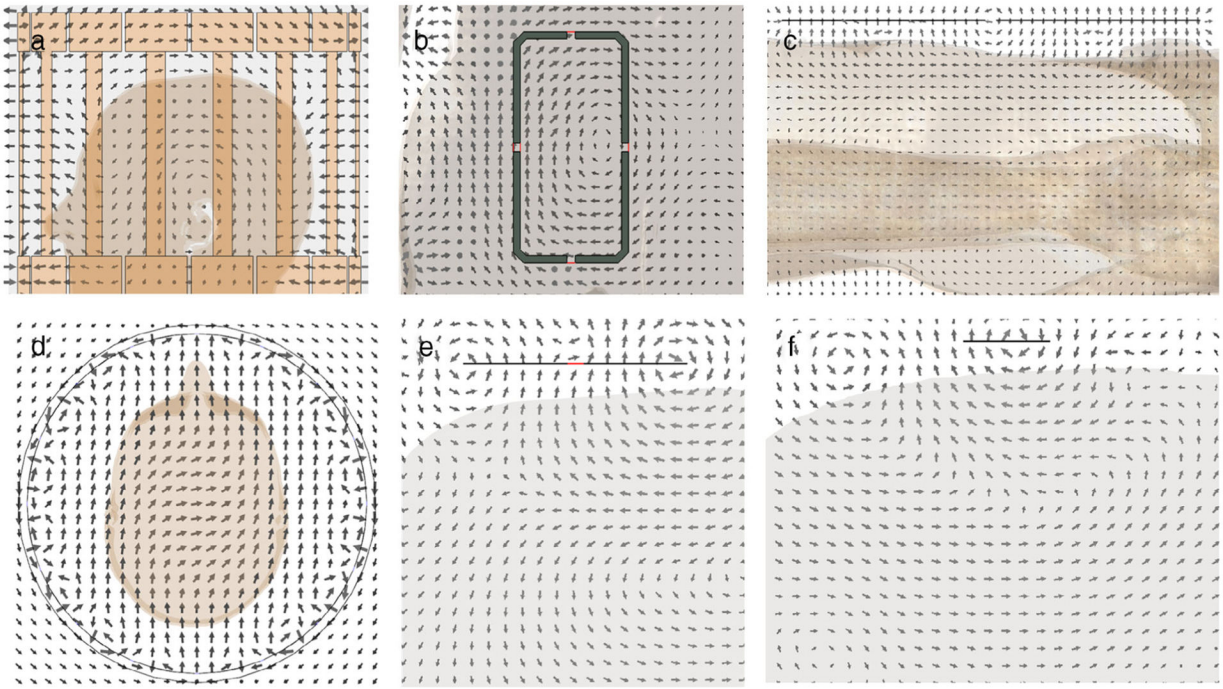

FIGURE 3:

Simulated representations of instantaneous field patterns for fundamental coil structures when loaded with a subject model. (**a**) Sagittal electric field pattern for birdcage coil. (**b**) Coronal electric field pattern for loop coil. (**c**) Sagittal electric field pattern for dipole antenna. (**d**) Transverse B_1-field pattern for birdcage coil. (**e**) Transverse B_1-field pattern for loop coil. (**f**) Transverse B_1-field pattern for dipole antenna.

FIGURE 4:
Commercially available RF coils for UHF MRI. (a) 2-channel birdcage transmit/receive coil with 32-channel receive array (Nova Medical, Wilmington, MA). (b) Birdcage transmit/receive wrist coil (Rapid Biomedical, Rimpar, Germany). (c) 16-channel transmit/receive cardiac loop coil array (MRI.Tools, Berlin, Germany)

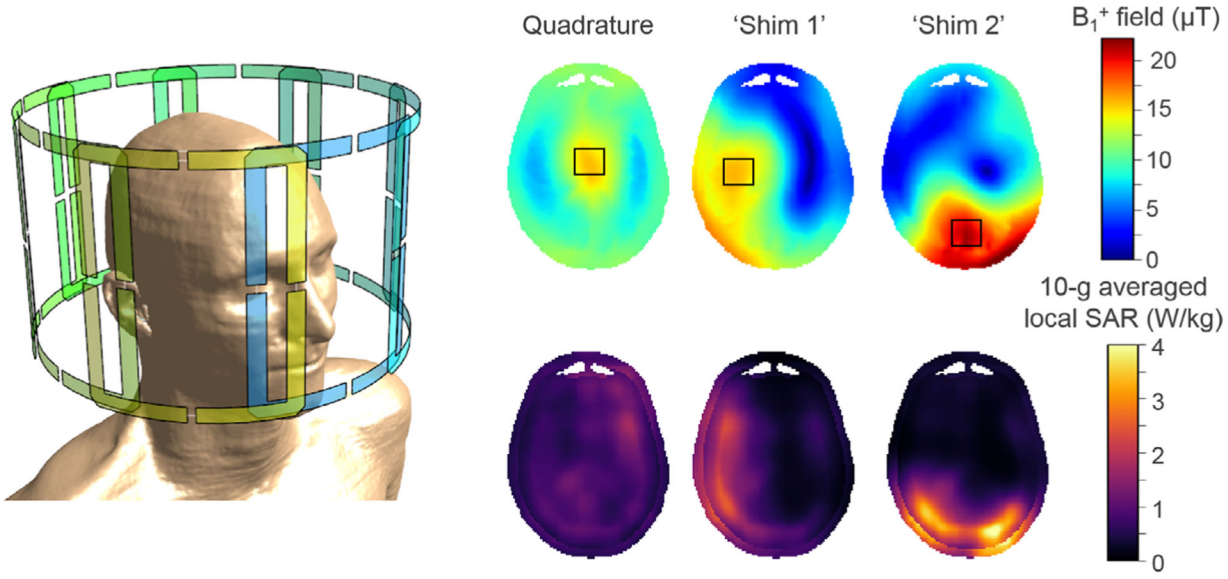

FIGURE 5:

Illustration of three simulated B_1^+ field and corresponding 10-g averaged local SAR distributions for an 8-channel transmit/receive head coil array using Finite Difference Time Domain (Sim4Life, ZMT, Switzerland). The phase settings of the individual drive channels determine the resulting B_1^+ field patterns; shown here are three distinct distributions resulting from a quadrature drive and two particular RF shim settings, although many more can be realized. The black squares indicate the focal region where B_1^+ fields are maximized. The corresponding local SAR distributions were calculated for a 1% duty cycle. RF phase settings can be used to steer the B_1^+ field distributions, but this also influences the local SAR distribution and therefore the potential level of tissue heating.

TABLE 1.

Comparison of the Maximum Magnetic Fields (B_0), Spatial Field Gradients (∇B_0), and Force Products ($B_0 \times \nabla B_0$)

System model (field strength)	$[B_0]_{max}$ [T]	$[\nabla B_0]_{max}$ [T/m]	$[B_0 \times \nabla B_0]_{max}$ [T^2/m]
OpenSpeed HFO (0.7T)[a]	1.5	25.2	34.6
OrthoOne(l.0 T)[a]	1.4	100.2	121.9
Panorama HFO (1.0 T)[b]	2.0	25.0	50.0
Achieva(1.5T)[b]	1.7	8.0	12.0
Aera (1.5 T)[c]	1.9	11.0	17.0
Achieva (3.0 T)[b]	—	17.0	48.0
Verio (3.0 T)[c]	3.4	10.0	27.0
Signa HDx (3.0 T)[a]	3.6	14.9	39.3
Magnetom Terra (7.0 T)[c]	7.2	12.2	61.0

Data in subject-accessible areas for a variety of open and horizontal bore system magnets. These positions of maximum fields typically occur within the bore or close to the bore opening for horizontal bore magnets. Note that the position of maximum magnetic field typically does not coincide with the position of maximum spatial field gradient.

[a]GE Healthcare.

[b]Philips Medical Systems.

[c]Siemens Medical Systems.